IJCRT.ORG ISSN : 2320-2882

INTERNATIONAL JOURNAL OF CREATIVE RESEARCH THOUGHTS (IJCRT)

An International Open Access, Peer-reviewed, Refereed Journal

Acacia Farnesiana Mediated Green Synthesis Of Silver Nanoparticles, Its Validation And Exploring Its Potential Against Lung Cancer – A549 Cell Lines

[1]Geethanjali R, [2]Kowsika G, [3]SathishKumar T, [4]Inbarasan E, [5]Shiney N S.

[1,2,3,4] Student, [5]Assistant Professor

[1,2,3,4,5]Pharmaceutical Technology,

[1,2,3,4,5]Gnanamani College of Technology, Namakkal, Tamilnadu, India

Abstract: In recent days, green synthesis of nanoparticles has gained attention due to its eco-friendly nature and biomedical applications. Conventional methods involve toxic chemicals, demanding sustainable alternatives for cancer treatment, particularly against drug-resistant lung cancer. Lung cancer remains a leading cause of mortality, necessitating novel, biocompatible, and cost-effective treatments. Silver nanoparticles synthesized using Acacia farnesiana offer a promising alternative with enhanced therapeutic efficacy and minimal toxicity. Analyzing existing studies, silver nanoparticles exhibit strong antimicrobial and anticancer potential. Green synthesis using plant extracts ensures eco-friendliness, cost-effectiveness, and biocompatibility. Acacia farnesiana-derived AgNPs show promising cytotoxicity against cancer cells, highlighting their potential in lung cancer therapy. Acacia farnesiana extract is prepared and mixed with silver nitrate ($AgNO_3$) solution. The reduction process is monitored via UV-Vis spectroscopy. The synthesized nanoparticles are characterized using FTIR, HPLC, GC-MS, XRD, FE-SEM, and EDX. Cytotoxicity is assessed through MTT assays on A549 lung cancer cells, with ROS generation and apoptosis studies confirming their mode of action. Statistical analysis validates their anticancer potential, ensuring reproducibility and accuracy. This research highlights a green, cost-effective approach for lung cancer treatment. Acacia farnesiana-mediated AgNPs exhibit biocompatibility, reducing side effects while enhancing therapeutic efficacy. Their cytotoxicity against A549 cells, stability, and apoptosis induction confirm their potential. Future work focuses on optimizing formulation for targeted drug delivery and in-vivo evaluation..

KEYWORDS **– Green synthesis, Silver nanoparticles, Acacia farnesiana, Lung cancer, A549 cell line, Cytotoxicity, Apoptosis.**

ABBREVIATIONS USED:

- AgNPs - Silver Nanoparticles
- $AgNO_3$ - Silver Nitrate
- UV-VIS – Ultra Violet Visible
- FTIR – Fourier transform Infrared spectroscopy
- HPLC – High Performance Liquid chromatography
- GCMS – Gas Chromatography -Mass Spectrometry
- XRD - X-ray Diffraction
- SEM - Scanning Electron Microscope
- EDAX – Energy Dispersive X-ray Analysis
- E.Coli – Escherichia coli

- S.Aureus – Staphylococcus Aureus
- C.albicans – Candida Albicans
- A549 cell line – Human Lung Adenocarcinoma Epithelial Cell line

I. INTRODUCTION

Lung cancer is a dominant cancer and with high morbidity and mortality rates worldwide. It hikes day by day and estimated that, about 10,000 new cases annually and also most deadly in both men and women, accounting for around 1,400,000 deaths each year. Green nanoparticles manufacturing with low toxicity has been a hot study field for biomedical applications such as implantable biomaterials, molecular imaging, wound healing, and drug delivery. Many variables, including smoking, a lack of physical activity, and food, can contribute to greater mortality rates from lung cancer. Because of the negative side effects, lung cancer treatment is typically limited to patients with severe diseases. Recently, physical, chemical, radiation therapy chemotherapy and surgical methods of the treatments are not better suitable. Development of cancer cells by drug resistant is a major reason for failure of drugs. Discovery and development of advanced drugs against cancer cell proliferation is facing great challenges due to side effects, toxicity and more cost efficiency. Due to this defect, the emerging need to discover novel, cost effective and bio-compatible therapeutic approaches against cancer cells are needed. Current clinical chemotherapies are non-selective. These anticancer medications are not completely degraded by human metabolism and enter the environment as effluents, impacting other eukaryotes. To try to overcome this problem, Plant Acacia Farnesiana mediated Ag NPs has indicated as a promising alternative solution to fight against cancer cells, without any side effects. Previous reports also supported to the plant A. Farnesiana has excellent potential biomedical agent with anti-microbial, anti-tumor, cytotoxic, anthelmintic, analgesic, anti-inflammatory, hypertensive, immune stimulatory and anti-cancer activities. Therefore, current study is focused on biosynthesize Ag NPs from A. farnesina and to evaluate its anti-cancer properties for lung cancer of A549 cells. AgNPs displayed significant cytotoxicity on A549 cells.

II. LITERATURE REVIEW

1.*Salfarina Ramli et al. (2011).*
The study "Antioxidant, Antimicrobial and Cytotoxicity Activities of Acacia farnesiana (L.) Willd. Leaves Ethanolic Extract" used ethanol Soxhlet extraction of Acacia farnesiana leaves. Antioxidant activity was evaluated using DPPH, reducing power, and metal chelating assays; antimicrobial activity by broth microdilution; and phytochemicals were analyzed using LC/MS and HPLC-PDA. The extract showed moderate antioxidant activity (EC50: 40.4 µg/mL), mild antibacterial activity only against Bacillus subtilis, poor antifungal activity, and was non-toxic in the brine shrimp assay at 1000 µg/mL.

2. *Vanlalvenia et al. (2021)*
The review titled "Green synthesis of silver nanoparticles using plant extracts and their antimicrobial activities" discusses the eco-friendly synthesis of silver nanoparticles (AgNPs) using plant-derived compounds. Phytochemicals such as flavonoids play a key role in reducing silver ions into nanoparticles, while the released Ag^+ ions exert antimicrobial effects by damaging bacterial cell structures. The study emphasizes that nanoparticle size, yield, and antibacterial efficiency are influenced by factors like plant extract concentration, silver nitrate levels, pH, and temperature.

3. *Anandalakshmi et al. (2016)*
The study "Characterization of silver nanoparticles by green synthesis method using Pedalium murex leaf extract and their antibacterial activity" reported the green synthesis of silver nanoparticles using Pedalium murex leaf extract. UV–Vis spectroscopy confirmed nanoparticle formation with a peak near 424 nm, while FTIR identified functional groups responsible for the reduction process. XRD analysis revealed their crystalline nature, and FESEM, TEM, and EDAX determined their size (20–50 nm), shape, and elemental composition. The synthesized nanoparticles exhibited strong antibacterial activity.

4. *Shan Tian et al. (2020)*
The study "Anti-cancer activity of biosynthesized silver nanoparticles using Avicennia marina against A549 lung cancer cells through ROS/mitochondrial damages" explored the cytotoxic potential of biosynthesized silver nanoparticles against A549 lung cancer cells. MTT assay results revealed strong dose-dependent anticancer activity, with 15% inhibition at 10 µg/mL and up to 94% at 80 µg/mL. Fluorescence microscopy

showed ROS generation and mitochondrial damage, indicating that oxidative stress led to cancer cell death as nanoparticle concentration increased.

III. Experimental materials & Methodology

3.1. Needed Materials and Reagents

Fig. 3.1 Acacia Farnesiana wild (L). Leaves

We gathered the fresh, healthy leaves of the Acacia Farnesiana shrub from the Salem District Herbarium Department in Tamil Nadu, India. Tap water was used to wash the samples, and then distilled water was used to remove any surface pollutants and diseased leaves. Reagents used 10% Folin–Ciocalteu reagent, 7.5% Sodium carbonate solution, Standard: Gallic acid (prepare standard curve) to analyse Phytochemicals. UV–Vis spectrophotometer (Cary 60, dual beam, 800–200 nm, 5 nm interval, 24000 nm/min). FTIR spectrometer (IRSpirit, 2 cm^{-1} resolution, 340–4700 cm^{-1} range, 45 scans, Happ-Genzel apodization) was used for Acacia Nano analysis. GC instrument Agilent 7890, Shimadzu – MODEL XRD 6,000, JEOL-MODEL-6390 microscopy. HIMEDIA Anti-bacterial antibiotic discs of narrow-spectrum and Broad spectrum were used. All the microbial cultures used in our study were purchased from the Microbial Type Culture Collection (MTCC), Chandigarh-160036, INDIA. The purchased bacterial strains include Staphylococcus aureus (MTCC96), Escherichia coli (MTCC1687),). The fungal cultures purchased include Candida albicans (MTCC 227). The human lung adenocarcinoma epithelial cell line, A549, were acquired from the National Centre for Cell Sciences (NCCS), Pune, India. With 10% (v/v) heat-inactivated fetal bovine serum (FBS), 100 U/mL penicillin, and 100 µg/mL streptomycin added, the cells were kept in the logarithmic phase of growth in Dulbecco's modified eagle medium (DMEM). They were kept in an incubator with 95% air humidity at 37°C and 5% CO_2.

3.2. Preparation of A.farnesiana hydralcoholic extract

The harvested leaves of A.farnesiana were air dried after which they were reduced to powdered form using mortar and pestle. The Soxhlet extraction begins by placing 25 g of dried herbal powder into filter paper and sealing it. This is then placed in a Soxhlet extractor connected to a round-bottom flask containing 150–300 mL of 90% ethanol and topped with a condenser. The ethanol is heated to evaporate, condense, and repeatedly wash the sample, extracting compounds over 6 hours. Once the solvent appears colorless, the setup is cooled and the extract is filtered. The solvent is removed using a rotary evaporator or water bath, and the dried extract is kept in a labeled container at 4 °C for further analysis.

Fig.3.2. Soxhlet extraction setup and Ethonolic extract collection

3.3. Phytochemical Analysis

Phytochemical analysis of Acacia farnesiana extract was performed to estimate total phenolic content using the Folin–Ciocalteu colorimetric assay. The test involved mixing 0.5 mL of the extract with 2.5 mL of 10% Folin–Ciocalteu reagreagentent, waiting for 5 minutes, and then adding 2.0 mL of 7.5% sodium carbonate. The mixture was incubated for 30 minutes in the dark at room temperature. Absorbance was measured at 765 nm. A standard curve was prepared using Gallic acid, and the phenolic content in the extract was calculated using the regression equation from this curve.

3.4. DPPH scavenging activity (Antioxidant activity)

The DPPH scavenging activity of the sample was measured by 1,1-diphenyl-2-picrylhydrazyl (DPPH) method (Manzocco et al., 1998). Briefly, 0.4mM solution of DPPH in methanol was prepared and 2 mL of this solution was added to different concentrations of sample and was allowed to stand at room temperature for 15 mins, and then absorbance was read at 517 nm against blank samples. Lower absorbance of the reaction mixture indicated higher free radical scavenging activity. The percentage of the DPPH radical scavenging is calculated using the equation as given below:

Radical scavenging activity/Inhibition (%) = (Abs control – Abs sample/ Abs control) x 100.

3.5. Green synthesis of silver nanoparticles with A.farnesiana

A stock solution of one molar silver nitrate ($AgNO_3$) was made. In order to prepare AgNPs, 0.1 mM $AgNO_3$ solution and leaf extract were extracted from that stock solution in a 5:1 ratio. 100 ml of 0.1 mM AgNO3 solution and 20 ml of leaf extract were combined, and the mixture was shaken in an Incubator set at 300 rpm and 37 °C for 48 hours. The solution's deep green hue gradually turned yellowish-brown, signifying that Ag+ was being converted to Ag0. Using a UV-VIS spectrophotometer, the impact of this silver nanoparticle production was observed. The spectrophotometric measurement was made at various points in time.

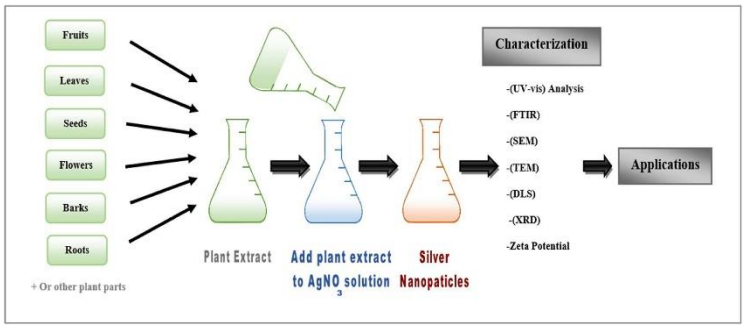

Fig.3.3. Synthesis of Silver Nanoparticles

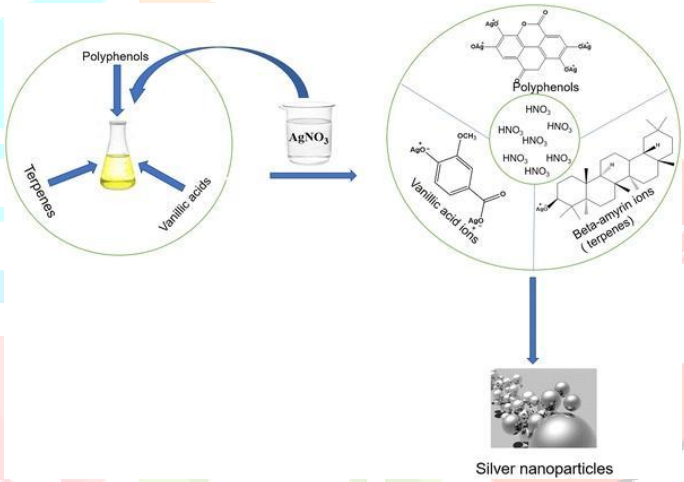

Fig.3.4. Mechanism of Silver Nanoparticles

3.6. Characterization of silver nanoparticles

Various analytical techniques were used for the characterization of green synthesized silver nanoparticles from A.farnesiana leaf extract. Constant monitoring of the reaction for the reduction of Ag+ ion by taking the OD (optical density) from 200–800 nm in a double beam UV–Vis spectrophotometer (Cary 60), FTIR, HPLC, GC-MS (Agilent 7890) equipped with phytochemical analysis. Further characterization of AgNPs was carried out through XRD, EDX equipped with size, crystal nature of NPs in a 2θ range from 20° to 80°. SEM analysis of derived nanoparticles was carried out with different levels.

3.6.1. UV visible Nanospectrophotometric Analysis

UV-Visible Nano spectrophotometry was used to analyze bioactive compounds like phenolics and flavonoids in Acacia farnesiana AgNPs extract. The spectrophotometer was first calibrated by selecting a wavelength range of 200–800 nm and blanking with solvent. The extract was dissolved in a suitable solvent (1 mg/mL), filtered, and placed in a quartz cuvette. A full wavelength scan was performed, and the maximum absorbance (λmax) was recorded. This peak indicates the presence of key phytochemicals in the sample.

3.6.2. FTIR Analysis of AgNPs

FTIR analysis was used to identify functional groups in the Acacia farnesiana dried extract. A small amount of sample (1–2 mg) was placed directly on the ATR crystal and pressed gently. The spectrum was collected (16–32 scans), saved, and the crystal was cleaned after use. Data was processed with baseline correction, and

key peaks were identified — such as O–H (~3300 cm^{-1}), C–H (~2920 cm^{-1}), C=O (~1700 cm^{-1}), and C=C (~1600 cm^{-1}). These peaks indicate the presence of phenols, alkanes, ketones, and aromatics in the extract.

3.6.3. High Performance Liquid chromatography (HPLC)

The crude Acacia farnesiana extract was analyzed using HPLC with a C18 column and methanol: water (80:20) as the mobile phase. The extract was dissolved in methanol, sonicated, filtered, and injected (10–20 µL) into the HPLC system. Separation was carried out at a flow rate of 1.0 mL/min, and detection was set at 230 nm. Chromatograms were recorded, and retention times and peak areas were analyzed to identify and compare phytochemical.

3.6.4. Gas Chromatography -Mass Spectrometry (GC-MS) Analysis

The Acacia farnesiana extract was analyzed by GC-MS to identify volatile and semi-volatile phytochemicals. The sample was dissolved in methanol or n-hexane, filtered, and injected (1 µL) into the GC-MS with an HP-5MS column and helium as the carrier gas. The oven temperature was programmed from 60°C to 280°C, and analysis lasted 30–40 minutes. The mass spectrometer operated in electron impact mode at 70 eV. Peaks were identified by comparing spectra with NIST libraries, and compounds were reported based on retention time and percentage peak area.

3.6.5. XRD Diffraction Analysis

The crystalline metallic silver was confirmed by XRD. The XRD measurement of bioreduced silver nanoparticles solution obtained was purified by repeated centrifugation at 10,000 rpm for 10 mins followed by redispersion of the pellet of silver nanoparticles in sterile distilled water. Further XRD instruments of the plant broths synthesized Ag nanoparticles solution were drop coted onto glass substrate and carried out on Shimadzu – MODEL XRD 6,000 operated at a voltage of 40 Kv and a current of a 30 A with Cu Kα radiation in a θ – 20 configurations.

3.6.6. FE-SEM Analysis

Scanning electron microscopy was carried out using a JEOL-MODEL-6390 microscopy. The dried silver nanoparticles were freeze dried and their structure was analyzed by SEM. Thin film of the sample was prepared on a carbon coated copper grid by just dropping a very small amount of sample on the sample grid, extra solution was removed using isolating aper and then the film on the SEM grid was allowed to dry putting it under a mercury lamp for 5 minutes. Each sample was analyzed by the scanning electron microscope (Khandelwal et al., 2010).

3.6.7. EDX Analysis

Energy dispersive X-ray spectrometers take advantage of the photon nature of light. In the X-ray range the energy of a single photon is just sufficient to produce a measurable voltage pulse X-ray, the output of an ultralow noise preamplifier connected to the low noise are a statistical measure of the corresponding quantum energy. By digitally recording and counting a great number of such pulses with in a so called Multi Channel Analyzer, a complete image of the X-ray spectrum is building up almost simultaneously. This digital quantum counting technique makes the energy dispersive spectrometry exceedingly reliable. A semiconductor material is used to detect the X-rays together with processing electronics to analyses the spectrum (Dinesh et al., 2012).

IV. ANTI-MICROBIAL ACTIVITY

The antimicrobial activity of Acacia farnesiana AgNPs extract was evaluated using the agar well diffusion method. Bacterial and fungal inoculums were prepared in Mueller Hinton broth and incubated for 24 hours at 37°C and 25°C, respectively. The agar plates were uniformly inoculated with the microbial cultures, and wells of 6 mm diameter were aseptically punched. A volume of 20–100 µL of the herbal extract was introduced into each well. After incubation under suitable conditions, the diameter of inhibition zones was measured. The results were compared with standard antibiotic discs, including narrow-spectrum, broad-spectrum, cutaneous, and subcutaneous types, to assess the extract's antimicrobial potential.

Fig 4.1 Microbial Inoculation

V. ANTI-CANCER ACTIVITY

The anticancer activity of the sample was tested against A549cell line by MTT (3-(4,5-dimethylthiazol-2-yl)-2,5-diphenyltetrazolium bromide assay (Mossman, 1983).The cells were seeded in 96-well microplates (1 x 10^4cells/well) and incubated at 37°C for 48 h in 5% CO_2 incubator and allowed to grow 70-80% confluence. Then the cells were treated with different concentrations of sample and incubated for 24 h. The morphological changes of untreated (control) and the treated cells were observed under digital inverted microscope (20X magnification) after 24 h and photographed. The cells were then washed with phosphate-buffer saline (PBS, pH-7.4) and 20 µL of (MTT) solution (5 mg/mL in PBS) was added to each well. The plates were then stand at 37ºC in the dark for 4 h. The formazan crystals were dissolved in 100 µL DMSO and the absorbance was read spectrometrically at 570 nm.

Percentage of cell viability was calculated using the formula,Cell viability (%) = (Absorbance of sample/Absorbance of control) X 100.

VI. RESULTS AND DISCUSSION

6.1. Phytochemical Analysis

The total phenolic content of Acacia farnesiana extract was determined using the Folin–Ciocalteu method at 765 nm. Based on the gallic acid standard curve, the extract showed a significant amount of phenolics, indicating strong antioxidant potential.

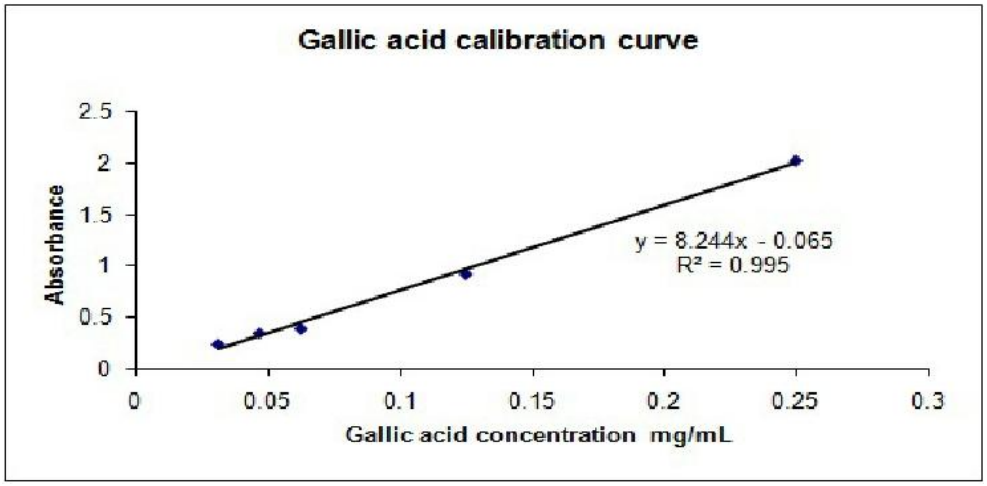

Fig.6.1 Gallic Acid Standard curve

Gallic Acid concentration (mg/l)	**Absorbance (Mean Value) at 765nm**
0.0312	0.241
0.0468	0.348
0.0625	0.393
0.123	0.922
0.26	2.021

Table 6.1. Absorbance of Standard Compound (Gallic Acid)

.

6.2. Green Synthesis of Silver Nanoparticles

The successful green synthesis of silver nanoparticles was visually confirmed by a distinct color change from pale yellow to dark brown after adding Acacia farnesiana extract to the silver nitrate solution. This transformation indicates the reduction of Ag^{+} ions to Ag^{0}, a key sign of nanoparticle formation. The dark brown coloration is attributed to surface plasmon resonance, characteristic of silver nanoparticles.

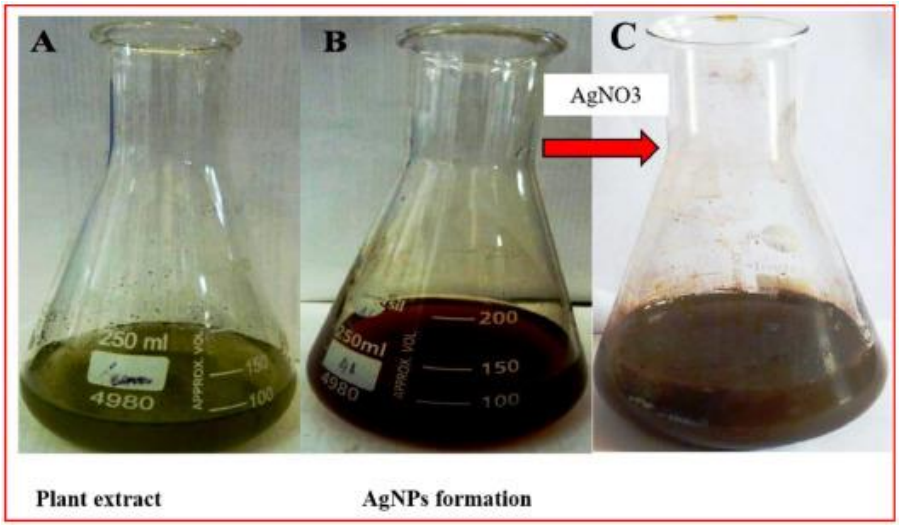

Fig 6.2. Formation of AgNPs

6.3. Characterization by UV-VIS Spectrophotometer.

The UV-Visible spectrophotometric analysis of Acacia farnesiana extract revealed a strong peak at 210 nm, indicating the presence of highly conjugated systems or aromatic phenolic structures. A distinct absorption at 230 nm corresponds to flavonoid compounds, particularly B-ring conjugation involving π→π* transitions. Additionally, the peak at 265 nm suggests the presence of polyphenols or tannins. These observations collectively confirm that the extract is rich in phenolic and flavonoid compounds, which are well-known for their antioxidant and antimicrobial properties.

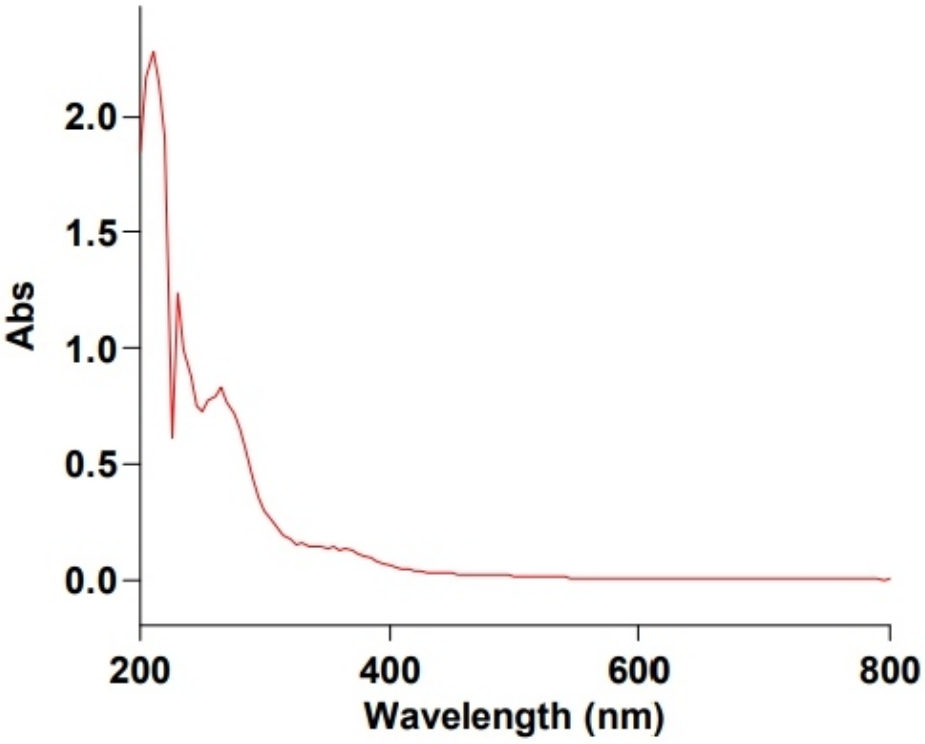

Fig 6.3. UV visible Spectrum

Table 6.2. Absorbance Vs Wavelength

Wavelength (nm)	**Absorbance**
265.0	0.832
230.0	1.234
210.0	2.276

6.4. Characterization by FTIR Analysis

The FTIR spectrum of Acacia farnesiana extract reveals key functional groups indicative of bioactive phytochemicals. The broad peak observed at 3332 cm^{-1} corresponds to O–H or N–H stretching vibrations, suggesting the presence of phenolic compounds or amines, which are characteristic of tannins and alkaloids. A sharp peak at 1636 cm^{-1} is attributed to C=C stretching, indicating the presence of aromatic rings commonly found in flavonoids or tannins. Additionally, the peak at 1013 cm^{-1} is associated with C–O stretching, which supports the presence of glycosides, ethers, or sugars. These spectral features collectively confirm the existence of bioactive constituents such as flavonoids, tannins, and phenolics, which contribute significantly to the medicinal properties of Acacia farnesiana.

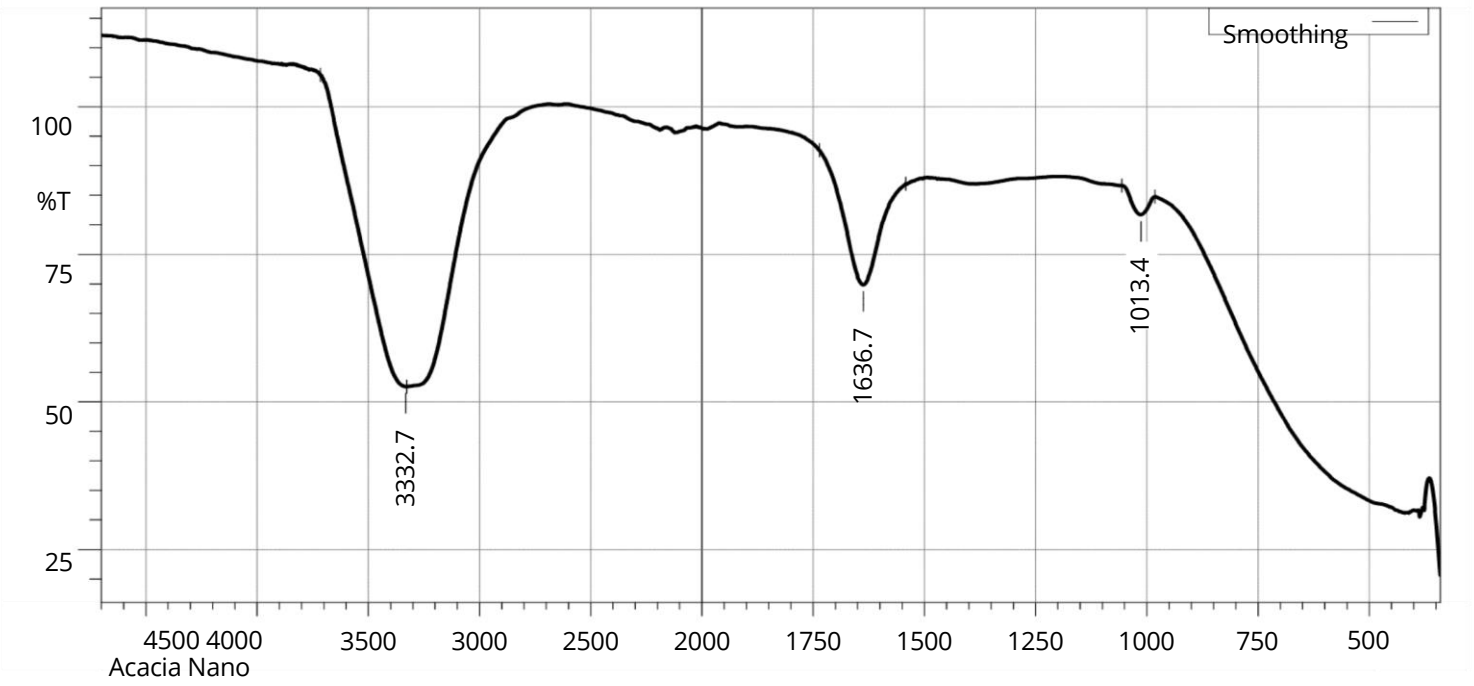

Fig 6.4. FTIR Spectrum

Table 6.3. FTIR Summary

Peak No.	Wavenumber (cm^{-1})	Intensity	Functional group
1	1013.43	81.71	C-O
2	1636.76	69.84	C=C
3	3332.71	59.54	C-H, N-H

6.5. Characterization by HPLC

Based on the HPLC chromatogram of the crude extract of Acacia farnesiana, several peaks were detected within a 10-minute retention time window. Below is an interpreted table summarizing the key features of the

chromatographic peaks, including approximate retention times and qualitative intensity levels based on peak height

The HPLC chromatogram of Acacia farnesiana reveals multiple well-defined peaks, indicating the presence of a diverse range of phytochemicals. A dominant peak observed at approximately 2.00 minutes suggests a high concentration of a polar, UV-active compound, likely a tannin or polyphenol, which are commonly found in Acacia species. Early eluting peaks between 1 to 3 minutes correspond to hydrophilic compounds such as phenolic acids and glycosides. In contrast, peaks appearing later between 4 to 7 minutes indicate the presence of less polar secondary metabolites, such as aglycones or alkaloids. This HPLC profile highlights the phytochemical richness of Acacia farnesiana and serves as a valuable tool for quality control, standardization, and potential compound isolation

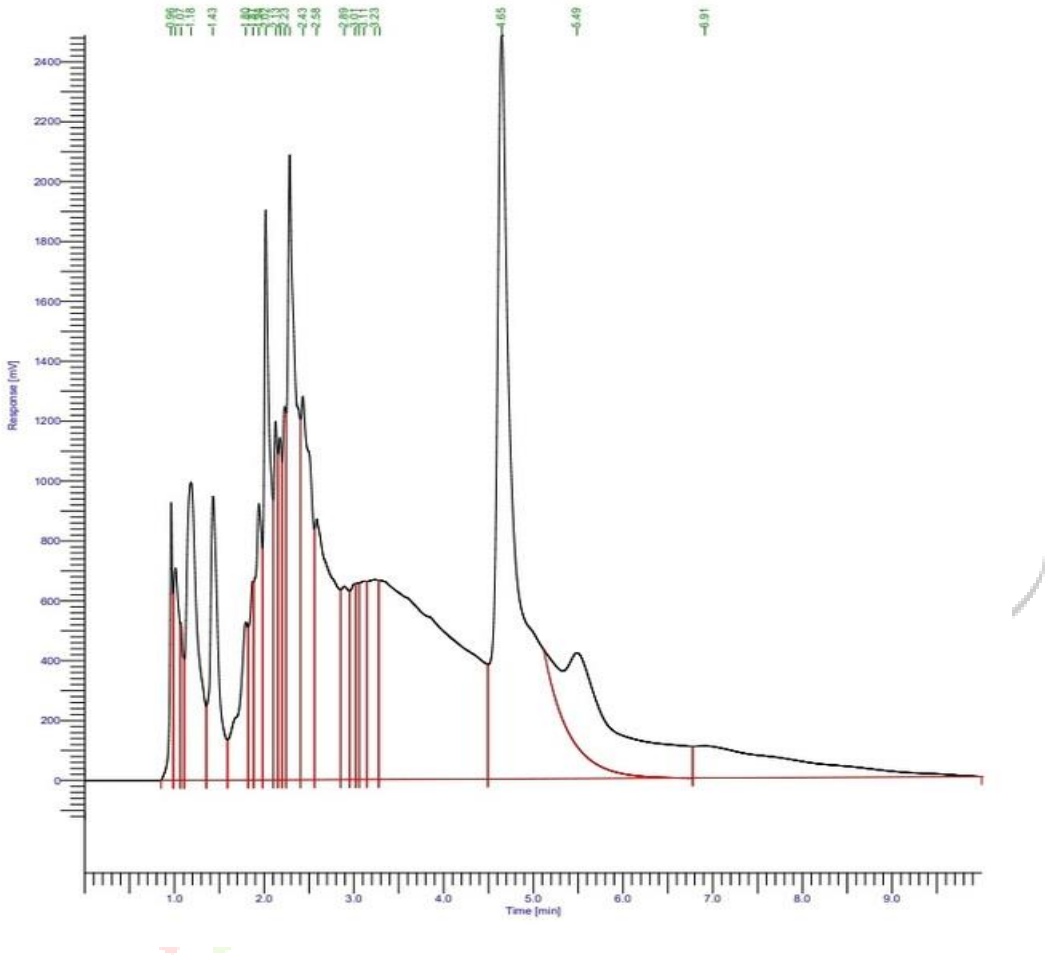

Fig 6.5. HPLC Peak Interpretation

Peak	Retention Time	Estimated Response	Interpretation
1	~1.00	Moderate (~600)	Polar phenolic compound
2	~1.80	High (~1800)	Flavonoid glycoside or tannin
3	~2.00	Very high (~2488)	Major compound-polyphenol
4	~2.50	Moderate (~1200)	Phenolic acid , Saponin.
5	~3.10	Moderate (~1000)	Flavonoid, aglycones
6	~4.69	Low (~400)	Less polar compound alkaloid
7	~5.65	Low (~300)	Minor metabolite
8	~6.91	Low (~250)	Late eluting compound lipophilic

Table 6.4. HPLC Peak Summary and Data

6.6. Characterization by GCMS Analysis

According to the GC/MS analysis, the hydro-alcoholic extract of A. farnesiana included at least 12 different chemicals. Using mass spectrometry coupled with GC, these chemicals were discovered. These chemicals' mass spectra were compared with those in the NIST/NBS spectral database, and the results are provided.

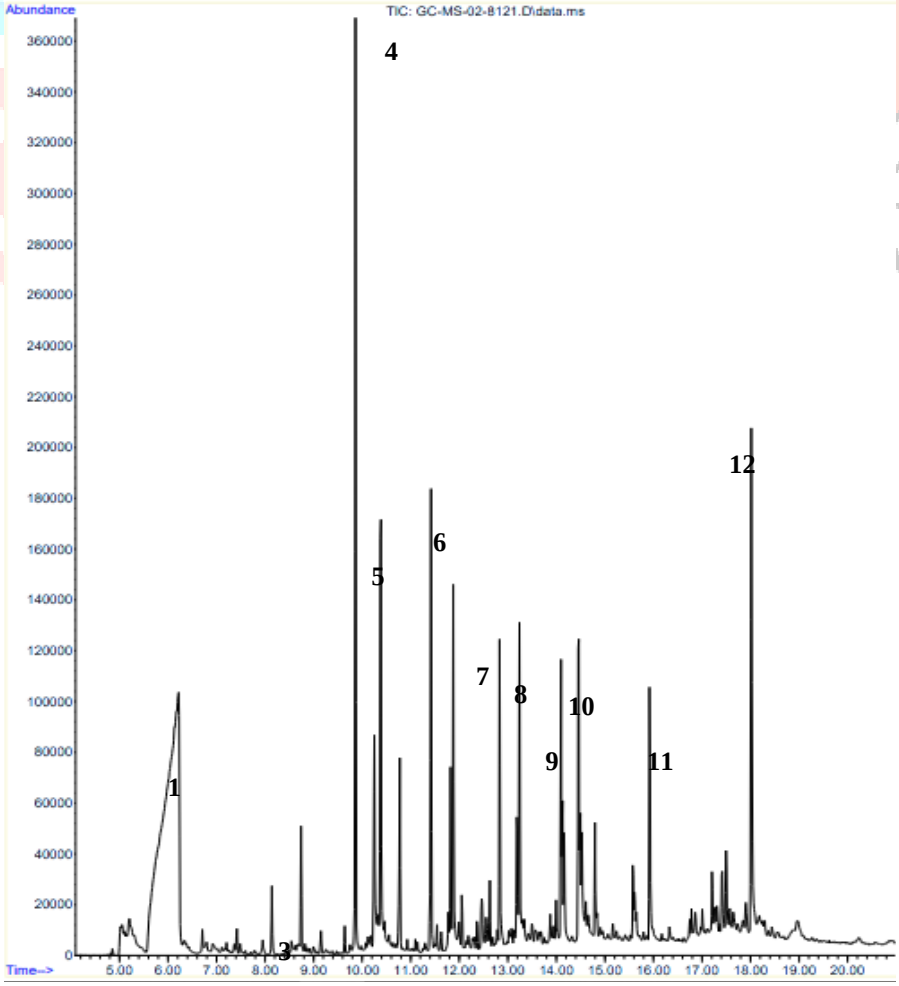

Fig 6.6. GC-MS Analysis Graph Interpretation

Table 6.5. GC- MS Peak Summary Interpretation

Peak no.	Interpretation
1	1-Butanol, 3-methyl,
2	4H-Pyran-4-one, 2,3-dihydro,
3	Thiophene, 2-propyl,
4	Thymol
5	Butonoic acid, 3-methyl
6	1,2,3, Benzenetriol
7	N- Phenylmaleimide,
8	Ethanone, 1-(2-hydroxy-4-methoxy
9	n-Hexadecanoic acid
10	n-Decanoic acid
11	Hexadecanoic acid, 2,3-dihydroxy,
12	Octadeconoic acid

According to research showing cytotoxicity, induction of apoptosis, and anti-proliferative activities, thymol was identified as the primary chemical with the fragmentation pattern (retention time 7.987) and possible anticancer actions in lung cancer. The next greater concentration at retention time 8.76 was 1,2,3-Benzenetriol, also referred to as Pyrogallol, which has also demonstrated possible anticancer characteristics. The retention period for n-hexadecanoic acid is 13.15. The retention time for the 4H-pyran-4-one, 2,3-dihydro, is 6.76. Butanoic acid, 3-methyl-N-phenylmaleimide, ethanol, 1-(2-hydroxy-4-methoxy), n-decanoic acid, hexadecanoic acid, 2,3-dihydroxy, octadecanoic acid, n-decanoic acid, 1-butanol, and 3-methyl compounds have already been reported to be present in the plant. These compounds have been found to have a variety of activities that may help protect against cancer.

6.7. Characterization by XRD

The X-ray diffraction (XRD) pattern of the prepared sample of silver nanoparticles was recorded by employing Bruker d8 Advance X-ray diffractometer, using CuKα radiation (λ = 1.5406 Å), 40 kV- 40mA, 2θ/θ scanning mode. Data was taken for the 2θ range of 10 to 100 degrees with a step of 0.0202 degree. The diffractogram (Fig. 1) showed two peaks at 2θ values of 21.52 and 23.87degree in the experimental diffractogram have been identified to be due to carbon nanoparticles and corresponding to (hkl) values – (002) and (100) planes of carbon. The XRD study has thus confirmed that the resultant particles in the prepared sample are carbon nanoparticles having crystalline structure.

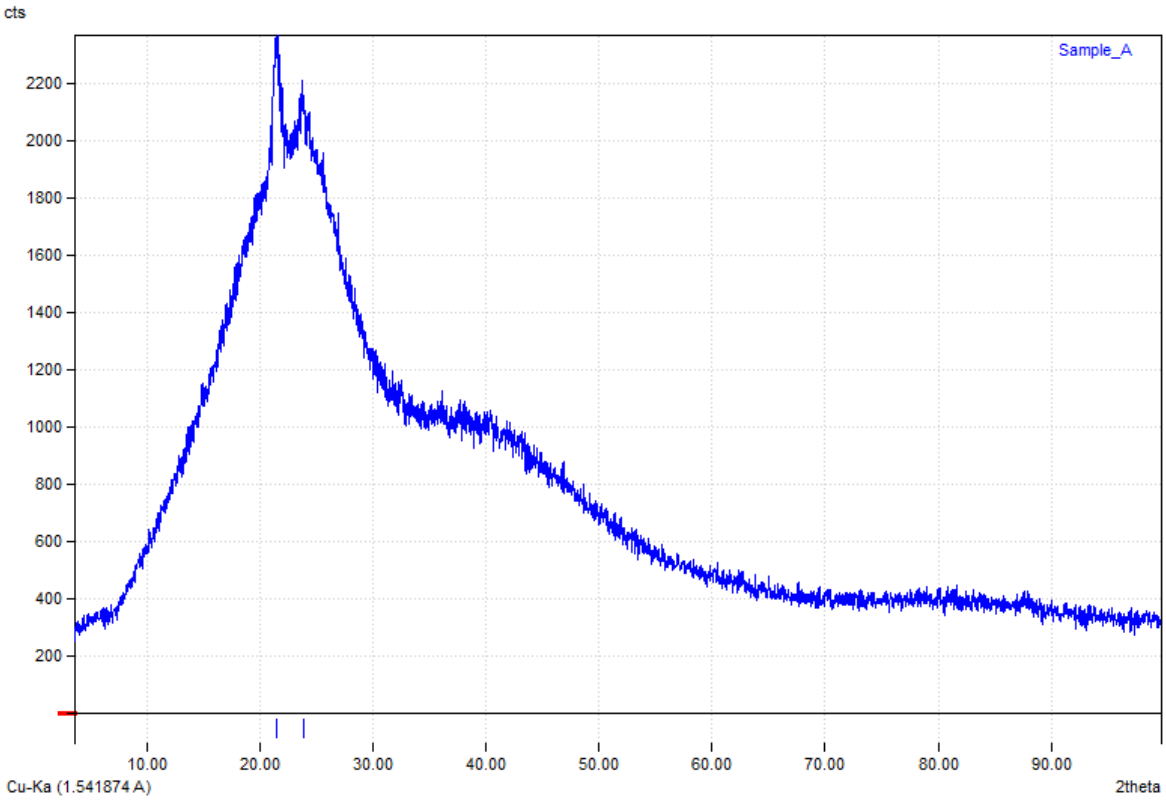

Fig .6.7. XRD Diffraction Analysis

6.8. Characterization by SEM

SEM revealed rough, crystalline carbon nanoparticles (10–18 nm) formed by molecular aggregation from plant-based synthesis.

- Top Left – 100 µm (Porous texture shows nanoparticle presence)
- Top Right – 50 µm (Nano-sized dots (10–18 nm) confirm fine synthesis)
- Bottom Left – 20 µm (Smooth spheres indicate uniformity)
- Bottom Right – 10 µm (Dense clumps suggest strong bonding)

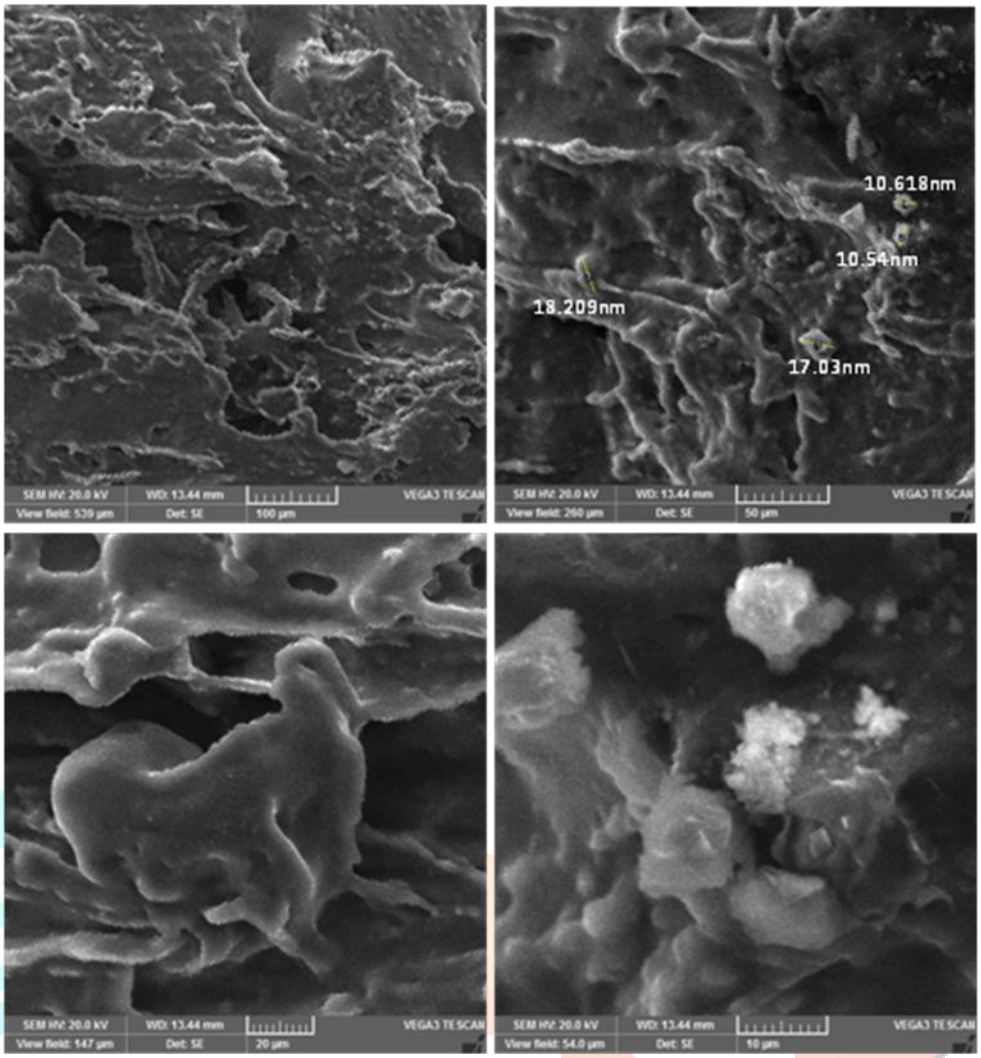

Fig.6.8. SEM Analysis

The 3D structure of silver nanoparticles has been elucidated using SEM image. The nanoparticles synthesized from plant extract were observed as rough surfaced irregular in nature as showed in Figure 6.8. It was shown that relatively crystalline carbon nanoparticles were formed with diameter of 10 to 18µm. The SEM image of carbon nanoparticles was due to aggregation of molecules bound to the nanoparticles.

6.9. Characterization by EDAX

EDX confirmed carbon dominance (72.63 wt%) with trace bio molecular elements, proving successful green synthesis and organic capping.

The presence of elemental carbon was confirmed by EDX analysis, the EDX profile showed in Figure 6.9. Carbon signal along with other weak signal which may have orientated from the biomolecules bound to the surface of nanoparticles shown in Table 6.6. It has been reported that nanoparticles synthesized using Green synthesis method was surrounded by a thin layer some capping organic materials from Acacia Farnesiana plant extract.

Table..6.6. EDAX Profile Summary

Element	Weight %	Atomic %
C K	72.64	79.44
O K	23.22	19.07
Al K	0.34	0.17
Cl K	1.53	0.57
K K	1.43	0.48
Ca K	0.85	0.28

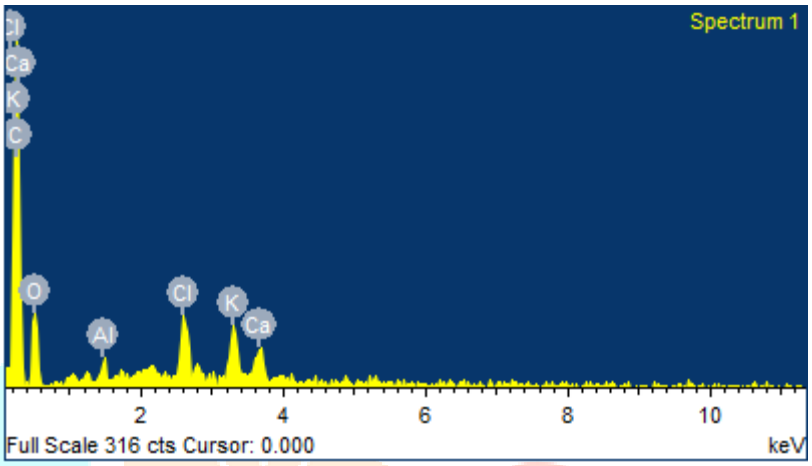

Fig.6.9. EDX Profile

- High carbon peak confirms core nanoparticle composition
- Minor O, K, Ca, Cl, and Al peaks suggest plant-derived bio-capping agents.
- Sharp signals validate elemental purity and green synthesis efficiency

6.10. Anti-Microbial Efficacy

The antimicrobial potential of Acacia farnesiana extract was assessed against Escherichia coli, Staphylococcus aureus, and Candida albicans using the agar well diffusion method. The zone of inhibition was measured in millimeters and the results are presented.

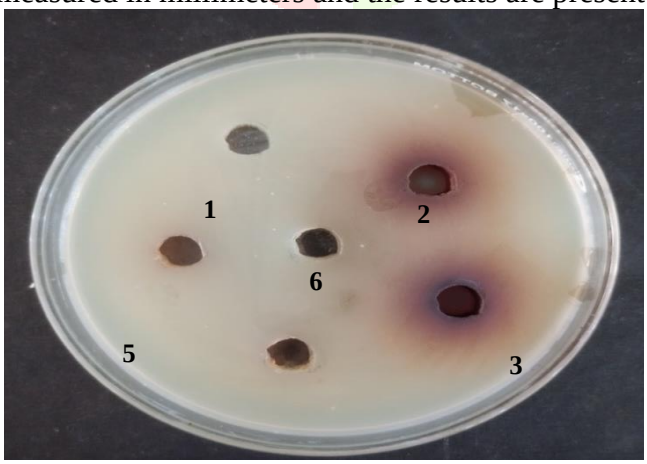

4

(A)

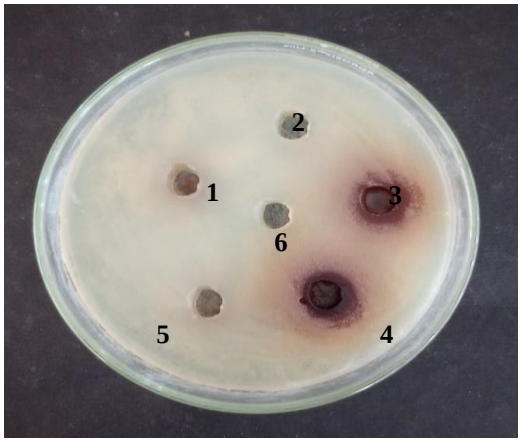

(B)

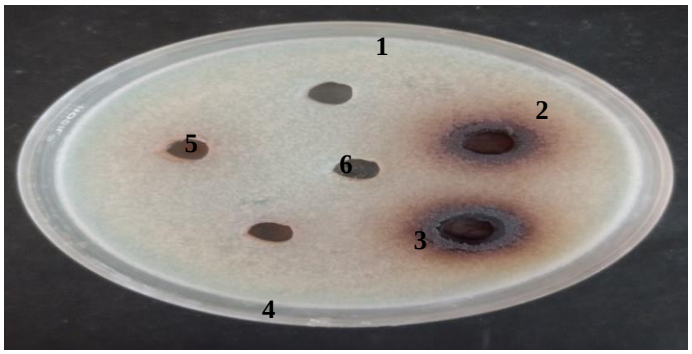

(C)

Fig.6.**10**. Antimicrobial activity (A) E.Coli, (B) S.Aureus, (C) C.Albicans

Table 6.7. AgNPs E.Coli

S.No	Bacteria E.Coli	
	Sample Name	Zone Measurement (mm)
1	AgNPs Stock Solution	No zone
2	Acacia Extract (50µl)	10mm
3	Acacia Extract (100µl)	14mm
4	AgNPs Sample (50µl)	10mm
5	AgNPs Sample (100µl)	No Zone
6	Negative Control	No zone

Table 6.8. AgNPs S.aureus Activity

S.No	Bacteria S.Aureus	
	Sample Name	Zone Measurement (mm)
1	AgNPs Stock Solution	No zone
2	Acacia Extract (50µl)	No zone
3	Acacia Extract (100µl)	12mm
4	AgNPs Sample (50µl)	10mm
5	AgNPs Sample (100µl)	15 mm
6	Negative Control	No zone

Table 6.9. AgNPs C.albicans Activity

S.No	Bacteria C.albicans	
	Sample Name	Zone Measurement (mm)
1	AgNPs Stock Solution	No zone
2	Acacia Extract (50µl)	No zone
3	Acacia Extract (100µl)	12mm
4	AgNPs Sample (50µl)	16mm
5	AgNPs Sample (100µl)	15 mm
6	Negative Control	No zone

- For E. coli, the extract showed moderate activity with a zone of 10 mm for 50 µL and 14 mm for 100 µL of crude extract. No zone was observed for the $AgNO_3$ stock, $AgNO_3$-synthesized nanoparticles, or negative control.
- Against S. aureus, zones of 10 mm and 12 mm were observed for 50 µL and 100 µL of extract, respectively. No inhibition was recorded for $AgNO_3$ or its synthesized nanoparticles.
- In the case of C. albicans, the extract demonstrated a stronger response with zones of 10 mm (50 µL) and 16 mm (100 µL), indicating some antifungal activity. However, no zones were found for $AgNO_3$ or synthesized samples.

These results are visually supported by the images provided in Figure 6.1 showing clear inhibition zones only around wells containing the plant extract.

6.11. Anti-cancer Activity

AgNPs' in vitro cytotoxicity was assessed using A549 cell lines at varying doses. A clear dose-response connection can be shown in our sample's cytotoxicity analysis, where cytotoxicity rose with increasing doses. Plotting the AgNP concentration on the X-axis against the cell viability percentage on the Y-axis allowed for the determination of the IC50 value. The A549 cell lines showed significant cytotoxicity from the materials. With an IC50 value of 20, 40, 60, 80, and 100 µg/ml, the results demonstrated that AgNPs strongly suppressed the growth of A549 cells, as indicated. AgNPs had an 84% inhibition rate on the cell line.

At control Treatment.

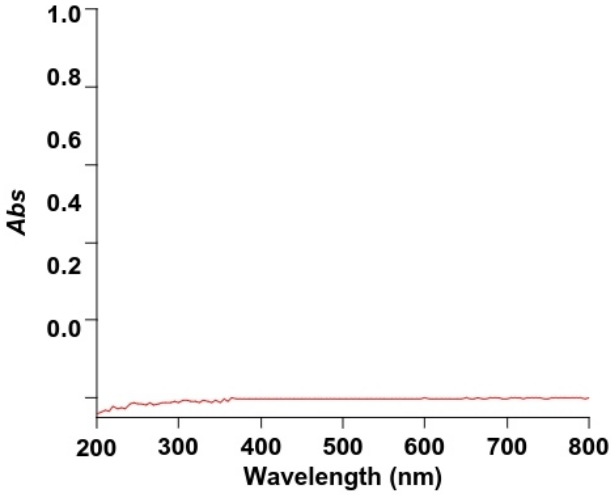

(A)

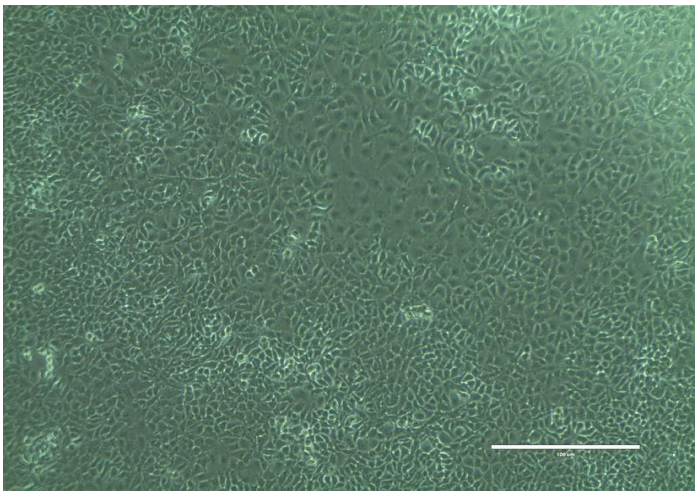

(B)

Fig 6.11. Anticancer Activity at Control
(A) Abs vs wavelength, (B) At Control treatment against

At 20,40,60,80µg/ml Treatment:

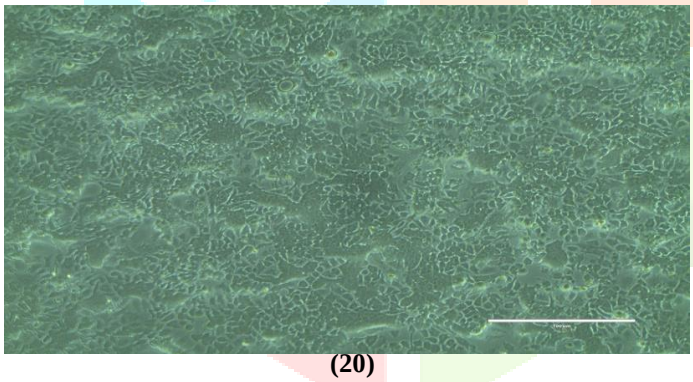

(20)

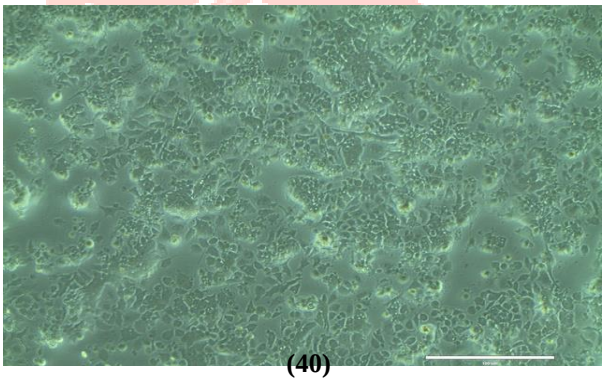

(40)

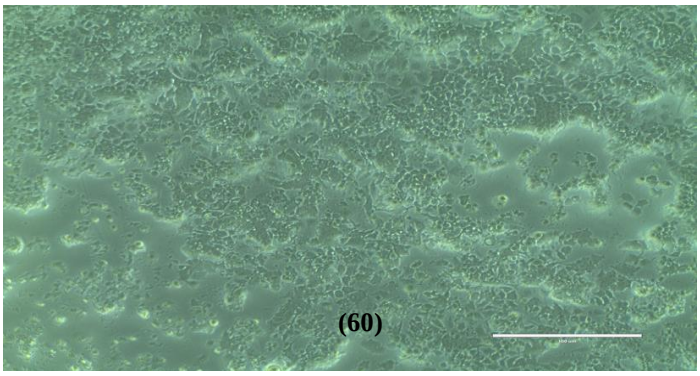

(60)

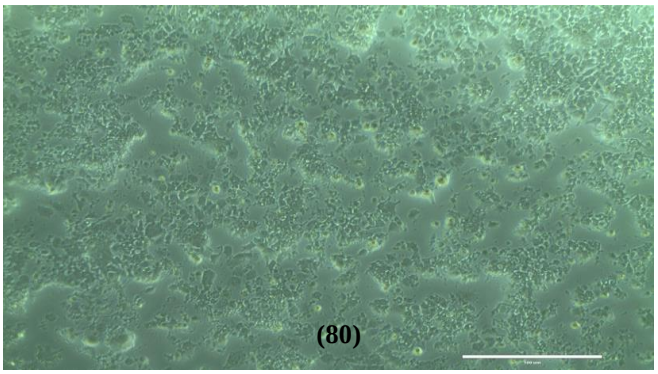

(80)

Fig. 6.12. Anticancer activity against A549 cell line at 20,40,60,80 µg/ml treated

At 100µg/ml Treatment:

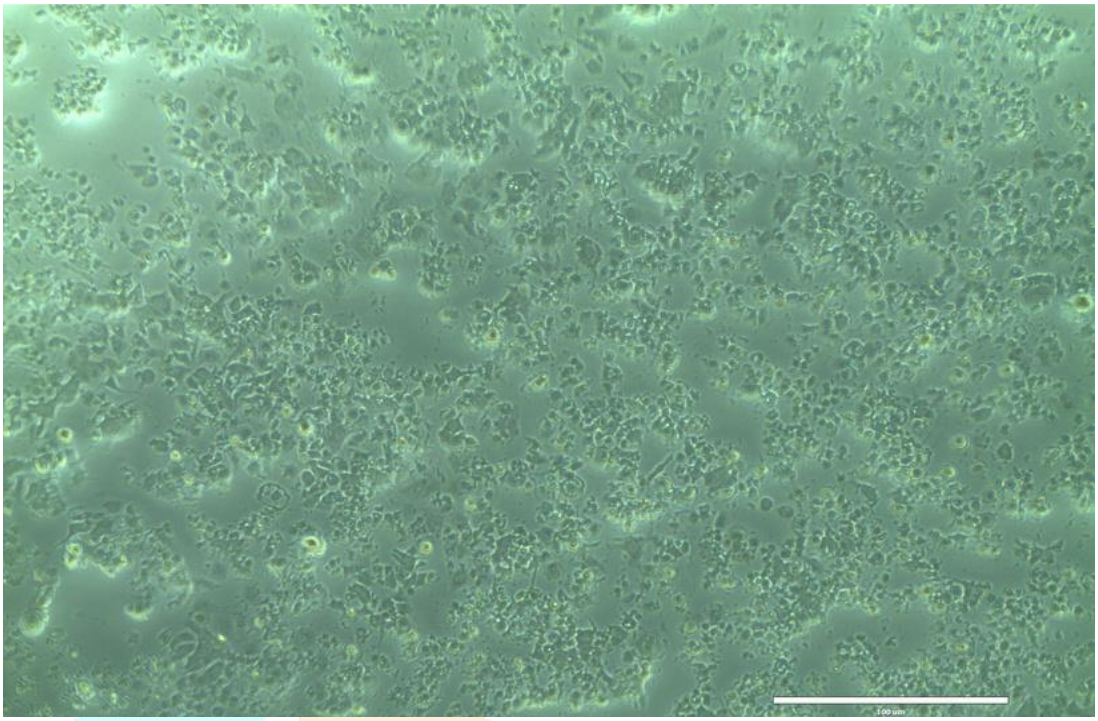

Fig.6.13. Anticancer activity at 100 µg/ml treatment

A549					
Concentrations (µg/ml)	Absorbance			Average	Cell Viability (%)
	I	II	III		
Control	0.822	0.817	0.823	0.820667	100
20	0.749	0.736	0.731	0.738667	90.00812348
40	0.565	0.562	0.558	0.561667	68.44029245
60	0.4	0.407	0.401	0.402667	49.06580016
80	0.208	0.21	0.216	0.211333	25.75142161
100	0.135	0.138	0.143	0.138667	16.89683184

Table 6.10. Cell Viability at Different concentrations

- Control showed full cell survival with no damage.
- Slight cell death observed, initial cytotoxic response at 20µg/ml treatment.
- Moderate cell death with noticeable reduction in viability at 40µg/ml treatment.
- Significant cell death suggesting enhanced nanoparticle effect at 60µg/ml treatment.
- Marked cytotoxicity with major loss of cell viability at 80µg/ml treatment.
- Severe cell death (84%) confirming strong anticancer activity at 100µg/ml treatment.

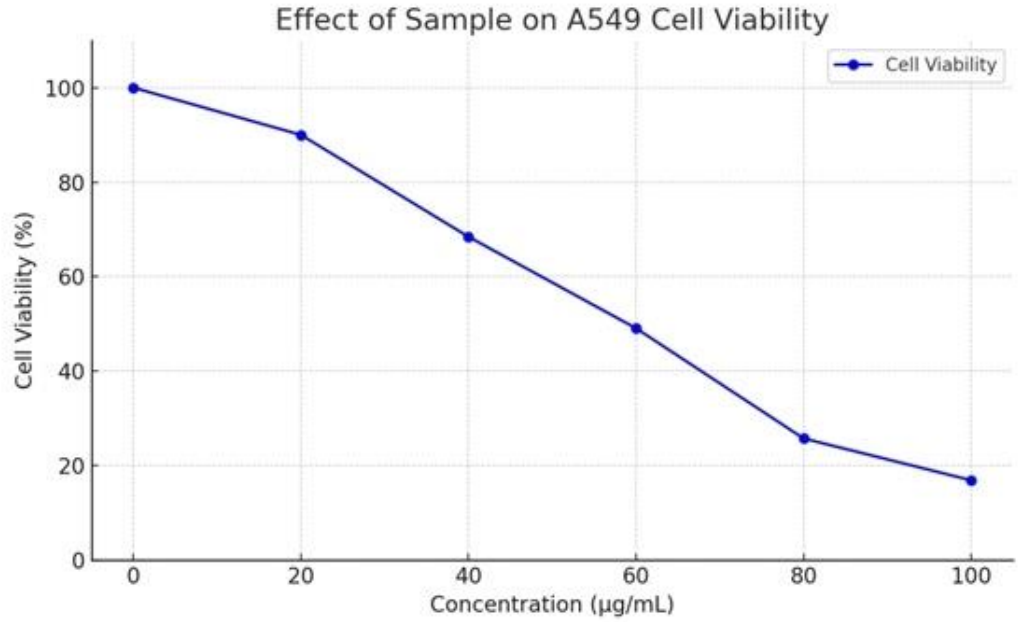

Graph showing the dose-dependent reduction in A549 cell viability with increasing sample concentration.

Fig. 6.14. Effect of sample on A549 cell Viability

The study assessed the anticancer potential of a test sample on the A549 human lung adenocarcinoma cell line using the MTT assay. Cells were treated with increasing concentrations of the sample (20 –100 µg/mL) and their viability was measured after 24 hours . Results show a clear dose -dependent cytotoxic effect. At the lowest concentration (20 µg/mL), cell viability remained high (90%), indicating minimal cytotoxicity. However, as concentration increased, cell viability significantly declined: 68.4% at 40 µg/ mL, 49.1% at 60 µg/mL, 25.8% at 80 µg/mL, and down to 16.9% at 100 µg/mL. This pattern suggests that the test sample exhibits strong anticancer activity by effectively inhibiting A549 cell proliferation in a dose -dependent manner. Morphological changes observed under the microscope likely confirm cell damage or apoptosis at higher doses. The IC50 value (concentration causing 50% inhibition) appears to fall between 40–60 µg/mL, underscoring the sample's potential as a cytotoxic agent against lung cancer cells. These findings warrant further investigation into its mechanism of action and potential therapeutic applications.

The biosynthesized silver nanoparticles showed efficient cytotoxicity against A549 lung cancer cells. A clear dose-dependent response was observed, with maximum cell death at 100 µg/mL. These findings suggest a promising anticancer potential of Acacia farnesiana-mediated nanoparticles.

VII. CHALLANGES AND POTENTIAL FUTURE WORK

AgNPs have a vast range of possible applications, and research into their synthesis utilizing green technology is expanding. Green nanoparticle production and phytochemicals obtained from plants can help create effective treatments for a number of fatal illnesses, including cancer. However, there are several difficulties in biotechnology because of the complexity and diversity of phytochemicals. Furthermore, AgNPs' surface charge, size, and shape primarily determine their biological activity, and these characteristics are difficult to manipulate throughout experimental methods. In order to examine their toxicity, mechanisms, and distribution, it is necessary to clarify their pharmacokinetics and pharmacodynamics. AgNPs may also be discharged into the environment, and this issue needs to be assessed. Nevertheless, the outcomes of in vitro research and in vivo trials differed. Therefore, more research is necessary to determine the toxicity of nanoparticles.

A further development in recent years has been the rise in the number of products that incorporate nanoparticles, primarily AgNPs. Therefore, research into AgNPs' toxicity to living things is crucial. Various methods have been devised; however, it is still unknown if AgNPs and antibiotics work in concert to combat

germs or the effectiveness of anticancer medicinal drugs. To fully comprehend the synergistic effects of the two distinct cytotoxic drugs, thorough research is required, taking into account the mechanism or mechanisms at play as well as the effectiveness of treatment. In order to cure various cancer, such efforts can aid in the development of innovative systems that employ a number of components. Therefore, identifying the primary source of nanoparticle-induced toxicity is crucial for creating safe and effective technologies and solutions.

VIII. CONCLUSION

With a focus on medicinal plant extracts, this research examines the latest advancements in the green synthesis, optimization conditions, mechanism, and characterisation methodologies for AgNPs. It also takes into account the impact of various parameters that influence green synthesis. The following is a detailed summary of this paper's primary contributions. Describe the latest advancements, processes, and mechanism for the environmentally friendly production of AgNPs. Talk about the many analytical methods available for characterizing AgNPs. Talk about the conditions for optimizing the green synthesis of AgNPs. Describe the most recent developments in the use of herbal plant-derived biosynthesized AgNPs as antibacterial, antifungal, and anticancer medicines. Talk about the difficulties and possible directions for future study in the green technology synthesis of AgNPs.

IX. ACKNOWLEDGEMENT

Sincere gratitude is extended by the authors to the Department of Pharmaceutical Technology at Gnananmani College of Technology, Namakkal, for providing the resources and assistance required to conduct this study. We also want to sincerely thank our project guide and the faculty for their invaluable support and direction during the project. A special thank you to the workers of our research center and lab technicians who helped with the cell line tests and characterization.

REFERENCES

[1] Yallappa, S., Manjanna, J., Peethambar, S.K. et al. Green Synthesis of Silver Nanoparticles Using Acacia farnesiana (Sweet Acacia) Seed Extract Under Microwave Irradiation and Their Biological Assessment. J Clust Sci 24, 1081–1092 (2013). https://doi.org/10.1007/s10876-013-0599-7

[2] T. Mossmann, Rapid colorimetric assay for cellular growth and survival: application to proliferation and cytotoxicity assays, J. Immunol. Methods. 65 (1983): 55–63. https://doi.org/10.1016/0022-1759(83)90303-4

[3] Dinesh S, Karthikeyan S and Arumugam P. (2012). Biosynthesis of silver nanoparticles from Glycyrrhiza glabra root extract. Archives of Applied Science Research, 4 (1):178-187 http://scholarsresearchlibrary.com/archive.html

[4] Tian, S., Saravanan, K., Mothana, R. A., Ramachandran, G., Rajivgandhi, G., & Manoharan, N. (2020). Anti-cancer activity of biosynthesized silver nanoparticles using Avicennia marina against A549 lung cancer cells through ROS/mitochondrial damages. Saudi Journal of Biological Sciences, 27(11), 3018–3024. https://doi.org/10.1016/j.sjbs.2020.08.029

[5] Erkovan, H. İ., Clarke, P. J., & Whalley, R. D. B. (2016). A review on General Description of Vachellia farnesiana (L.) Wight &Arn. Atatürk Üniversitesi Ziraat Fakültesi Dergis

[6] Rafique, M., Sadaf, I., Rafique, M. S., & Tahir, M. B. (2016). A review on green synthesis of silver nanoparticles and their applications. Artificial Cells, Nanomedicine, and Biotechnology, 45(7), 1272–1291. https://doi.org/10.1080/21691401.2016.1241792

[7] Zarfishan Zulfiqar, Rana Rashad Mahmood Khan, Muhammad Summer, Zohaib Saeed, Muhammad Pervaiz, Shahzad Rasheed, Behram Shehzad, Fatima Kabir, Saira Ishaq. "Plant-mediated green synthesis of silver nanoparticles: Synthesis, characterization, biological applications, and toxicological considerations: A review." Biocatalysts and Agricultural Biotechnology, vol. 57, 2024, https://doi.org/10.1016/j.bcab.2024.103121.

[8] Mohd Fahim, Adnan Shahzaib, Nahid Nishat, Afroz Jahan, Tahir Ahmad Bhat, Afreen Inam. "Green synthesis of silver nanoparticles: A comprehensive review of methods, influencing factors, and applications." JCIS Open, vol. 16, 2024, https://doi.org/10.1016/j.jciso.2024.100125.

[9] Ramli, Salfarina, Harada, Ken-ichi, & Ruangrungsi, Nijsiri. (2011). Antioxidant, antimicrobial and cytotoxicity activities of Acacia farnesiana (L.) Willd. Leaves ethanolic extract. Pharmacognosy Journal, 3(23), 50–58. https://doi.org/10.5530/pj.2011.23.8

[10] Khandelwal K R. (2010). Practical Pharmacognosy Techniques and Experiments. 15th ed. Pune, Nirali Prakashan; 15–163.

https://books.google.co.in/books?hl=en&lr=&id=SgYUFD_lkK4C&oi=fnd&pg=PA1&dq=info:kQBbjR8LdrkJ:scholar.google.com/&ots=SfbXqsky4N&sig=XiUSPtXe03XpqIdmJ8GAOClglkk&redir_esc=y#v=onepage&q&f=false

[11] Vijay Kumar, P. P. N., Pammi, S. V. N., Kollu, P., Satyanarayana, K. V. V., & Shameem, U. (2014). Green synthesis and characterization of silver nanoparticles using Boerhaavia diffusa plant extract and their antibacterial activity. Industrial Crops and Products, 52, 562–566. https://doi.org/10.1016/j.indcrop.2013.10.050

[12] Njud S. Alharbi, Nehad S. Alsubhi, Afnan I. Felimban. "Green synthesis of silver nanoparticles using medicinal plants: Characterization and application." Journal of Radiation Research and Applied Sciences, vol. 15, no. 3, 2022, https://doi.org/10.1016/j.jrras.2022.06.012.

[13] Samuel, M. S., Ravikumar, M., John, J. A., Selvarajan, E., Patel, H., Chander, P. S., Soundarya, J., Vuppala, S., Balaji, R., & Chandrasekar, N. (2022). A review on green synthesis of nanoparticles and their diverse biomedical and environmental applications. Catalysts, 12(5), 459. https://doi.org/10.3390/catal12050459

[14] Saleema, N.H., Abdelhalimb, A.R., Alghoulc, A.M. and Abdel-Rhmanb, S.H., 2023. In-vitro antimicrobial activity of Acacia farnesiana & Rosmarinus officinalis crude extract and isolated compounds against foodborne pathogens.DOI: https://doi.org/10.56293/IJMSSSR.2022.4653

[15] Green Route Synthesis and Characterization Techniques of Silver Nanoparticles and Their Biological Adeptness, Nitin Kumar Sharma, Jyotsna Vishwakarma, Summi Rai, Taghrid S. Alomar, Najla AlMasoud, and Ajaya Bhattarai, ACS Omega 2022 7 (31), 27004-27020: DOI: 10.1021/acsomega.2c0140

[16] Koregol, A.C., Kalburgi, N.B. and Kotecha, A.K., 2016. Acacia catechu and Acacia farnesiana as antimicrobial agents against periodontal pathogens: An in vitro assessment. Journal Of Applied Dental and Medical Sciences, 2, p.3. https://doi.org/10.56293/IJMSSSR.2022.4653.

[17] Yang, S. (2021). Characterization of Silver Nanoparticles. In: Lal, H.M., Thomas, S., Li, T., Maria, H.J. (eds) Polymer Nanocomposites Based on Silver Nanoparticles. Engineering Materials. Springer, Cham. https://doi.org/10.1007/978-3-030-44259-0_4

[18] Jain, N., Jain, P., Rajput, D. Et al. Green synthesized plant-based silver nanoparticles: therapeutic prospective for anticancer and antiviral activity. Micro and Nano Syst Lett 9, 5 (2021). https://doi.org/10.1186/s40486-021-00131-6

[19] Anandalakshmi, K., Venugobal, J. & Ramasamy, V. Characterization of silver nanoparticles by green synthesis method using Pedalium murex leaf extract and their antibacterial activity. Appl Nanosci 6, 399–408 (2016). https://doi.org/10.1007/s13204-015-0449-z

[20] Vanlalveni, Chhangte Lallianrawna, Samuel Ayushi Selvaraj, Manickam Changmai, Bishwajit Rokhum, Samuel Lalthazuala, Green synthesis of silver nanoparticles using plant extracts and their antimicrobial activities: a review of recent literature, 2021. https://doi.org/10.1039/rsc_crossmark_policy

[21] Greenwell, M., & Rahman, P. K. (2015). Medicinal Plants: Their Use in Anticancer Treatment. International journal of pharmaceutical sciences and research, 6(10), 4103–4112. https://doi.org/10.13040/IJPSR.0975-8232.6(10).4103-12

[22] Devi, J.S., Bhimba, B.V. and Ratnam, K., 2012. In vitro anticancer activity of silver nanoparticles synthesized using the extract of Gelidiella sp. Int J Pharm Sci, 4(4), pp.710-715.

[23] Pirsaheb, M., Gholami, T., Seifi, H. Et al. Green synthesis of nanomaterials by using plant extracts as reducing and capping agents. Environ Sci Pollut Res 31, 24768–24787 (2024). https://doi.org/10.1007/s11356-024-32983-x

[24] Mohamad, N.A.N., Arham, N.A., Jai, J., Hadi, A., 2013. Plant Extract as Reducing Agent in Synthesis of Metallic Nanoparticles: A Review. AMR 832, 350–355. https://doi.org/10.4028/www.scientific.net/amr.832.350

[25] Arshad, F., Naikoo, G.A., Hassan, I.U. et al. Bioinspired and Green Synthesis of Silver Nanoparticles for Medical Applications: A Green Perspective. Appl Biochem Biotechnol 196, 3636–3669 (2024). https://doi.org/10.1007/s12010-023-04719-z

[26] Gomes, H. I. O., Martins, C. S. M., & Prior, J. A. V. (2021). Silver Nanoparticles as Carriers of Anticancer Drugs for Efficient Target Treatment of Cancer Cells. Nanomaterials, 11(4), 964. https://doi.org/10.3390/nano11040964